Research Journal of Applied Sciences, Engineering and Technology 5(11): 3219-3225, 2013
ISSN: 2040-7459; e-ISSN: 2040-7467

Submitted: October 17, 2012 Accepted: December 10, 2012 Published: April 05, 2013

Surface Reconstruction from Sparse and Arbitrarily Oriented Contours in Freehand 3D Ultrasound

[1, 2]Shuangcheng Deng, [1]Yunhua Li, [2]Lipei Jiang, [2]Yingyu Cao and [2]Junwen Zhang
[1]School of Automation Science and Electrical Engineering, Beijing University of Aeronautics and Astronautics, Beijing, China
[2]Opto-Mechatronic Equipment Technology Beijing Area Major Laboratory, Beijing Institute of Petrochemical Technology, Beijing, China

Abstract: 3D reconstruction for freehand 3D ultrasound is a challenging issue because the recorded B-scans are not only sparse, but also non-parallel (actually they may arbitrarily orient in 3D space and may intersect each other). Conventional volume reconstruction methods can't reconstruct sparse data efficiently while not introducing geometrical artifacts and conventional surface reconstruction methods can't reconstruct surfaces from contours that are arbitrarily oriented in 3D space. We developed a new surface reconstruction method for freehand 3D ultrasound based on variational implicit function which is presented by Greg Turk for shape transformation. In the new method, we first constructed on- and off-surface constraints from the segmented contours of all recorded B-scans and then used a variational interpolation technique to get a single implicit function in 3D. Finally, the implicit function was evaluated to extract the zero-valued surface as final reconstruction result. Two experiments was conducted to assess our variational surface reconstruction method and the experiment results have shown that the new method is capable of reconstructing surface smoothly from sparse contours which can be arbitrarily oriented in 3D space.

Keywords: Freehand 3D ultrasound, medical imaging, surface reconstruction, variational method

INTRODUCTION

Freehand 3D ultrasound imaging uses conventional ultrasound technology to build up a 3D data set from a number of conventional 2D B-scans acquired in succession. It consists of tracking a standard 2D ultrasound probe by using a 3D localizer (magnetic, mechanical or optic). The localizer is attached to the probe and can continuously measure the 3D position and orientation of the probe while the physician moves the probe slowly and steadily over a particular anatomical region. The measured outputs of the 3D positions and orientations are used for the localization of B-scans in the coordinate system of the localizer. In order to establish the transformation between the B-scan coordinates and the 3D position and orientation of the probe, a calibration procedure is necessary (Fenster and Downey, 1996; Rousseau *et al*., 2005, 2006).

There are two main drawbacks of freehand imaging: The first is that the recorded B-scans are non-parallel in 3D space, actually they may arbitrarily oriented in 3D and may intersect each other, because the movement of the ultrasound probe is unrestricted. The second is that the recorded B-scans are very sparse. This arise from the fact that it would be an advantage to reconstruct from a smaller number of ultrasound contours, since manual segmentation, which is still the only universally reliable method for ultrasound data (Gopal *et al*., 1997), is the most time consuming part of the processes involved. So only a small number of B-scans are recorded and manually segmented in order to allow real-time response in clinic applications. These two drawbacks make the 3D reconstruction of the ultrasound data quite complex.

All the reconstruction methods for freehand 3D ultrasound fall into two categories: volume reconstruction and surface reconstruction. Volume Reconstruction methods interpolate the data to a regular 3D array (voxel array). The most common volume reconstruction methods are Pixel Nearest-Neighbor (PNN) (Nelson and Pretorius, 1997), Voxel Nearest-Neighbor (VNN) (Prager *et al*., 1999; Sherebrin *et al*., 1996) and Distance-Weighted interpolation (DW) (Barry *et al*., 1997; Trobaugh *et al*., 1994). All these volume reconstruction methods can't reconstruct sparse data efficiently while not introducing geometrical artifacts, degrading or distorting the images. So they are only suitable for the reconstruction of dense data and are not a feasible choice for our case.

Surface Reconstruction methods reconstruct the VOI (volume of interest) directly from contours (cross-

Corresponding Author: Shuangcheng Deng, School of Automation Science and Electrical Engineering, Beijing University of Aeronautics and Astronautics, Beijing, China

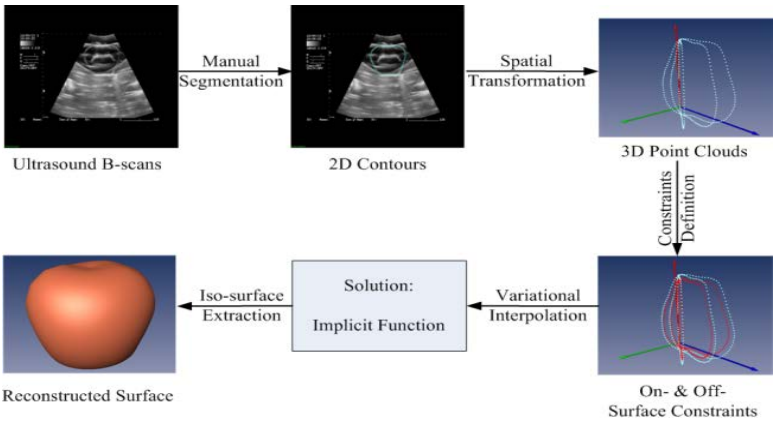

Fig. 1: Process of new surface reconstruction method

sections) segmented from the original ultrasound B-scans in a prerequisite step. These B-scans do not contain processing artifact, hence the clinician has a better chance of outlining the contours of the organ accurately.

Nowadays methods that can handle arbitrarily oriented and mutually intersected contours are few and far between. Most of surface reconstruction methods mentioned in literature directly triangulate between two adjacent contours and can't handle arbitrarily oriented contours. Usually the contours are nearly parallel and don't intersect each other (Gopal *et al*., 1997; Cook *et al*., 1980; King *et al*., 1994; King *et al*., 1994; Hodges *et al*., 1994). Liu *et al*. (2008) and Altmann *et al*. (1997) proposed a method to reconstruct non-parallel contours. It is also done directly in the surface-mesh (i.e., triangle-mesh) domain and requires dense contours for input. It is also incapable of reconstructing sparse data in our case.

We develop a new surface reconstruction method for freehand ultrasound imaging. It is based on variational interpolation, which is used by Turk *et al*. (2001) for shape transformation (Liu *et al*., 2008). It can effectively solve the surface reconstruction of the physical organ and can handle both sparse and mutually intersected contours data.

PROCESS OF SURFACE RECONSTRUCTION FOR FREEHAND 3D ULTRASOUND IMAGING

Our new surface reconstruction method is based on variational interpolation. It casts the surface reconstruction problem to an equivalent variational problem which tries to find a function that has minimum bending energy and satisfies all constraints. The process of this method is illustrated in Fig. 1.

First, we perform a spatial transformation to convert the 2D pre-segmented ultrasound contours into 3D point clouds, which casts the surface reconstruction problem as a scattered data interpolation problem in three dimensions. The spatial transformation is performed according to the 3D position and orientation information of the ultrasound probe while acquiring corresponding 2D ultrasound B-scans. Contours are manually segmented from the original B-scans in a prerequisite step.

Secondly, we define all the boundary points of the ultrasound contours as on-surface constraints for the scattered data interpolation problem in three dimensions. For unambiguously defining the solution function, we define additional constraints that indicate which points should be located inside the object. These are off-surface constraints for the scattered data interpolation.

Thirdly, variational interpolation is invoked to solve the scattered data interpolation, the solution is a single implicit function in 3D that will be at least C1-continuous, i.e., it is smooth.

Finally, an iso-surface extraction step is performed. The implicit function is evaluated to extract the zero-valued surface as the reconstruction result. The iso-surface extraction algorithm used in our study is the Marching Cubes algorithm proposed by William and Harvey (1987).

VARIATIONAL SURFACE RECONSTRUCTON

- **Constraints definition:**
  On-surface constraints: All the contour points are considered as on-surface constraint points and will lie exactly on the surface that will be reconstructed. Hence, each on-surface is assigned a scalar value 0.

Off-surface constraints: In order to unambiguously define the solution function, we need some additional off-surface constraints that define which points should be located inside the object. In this study we define some additional normal constraints which are known to be inside the reconstructed surface as off-surface constraints.

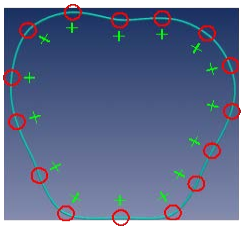

Fig. 2: Pairs of on- and off- surface constraints (circles and pluses)

The location of a normal constraint c^N_i (or off-surface constraint c^{off}_i) is calculated by adding a on-surface constraint c^{on}_i to the normal n_i at that point, that is:

$$c^{off}_i = c^N_i = c^{on}_i + n_i \quad (1)$$

So each off-surface constraint is paired with a corresponding on-surface constraint and the number of off-surface constraints is equal to that of on-surface constraints. Figure 2 shows some defined on- and off-surface constraints. The point cloud of on- and off-surface constraints is passed to the following variational interpolation routine. While contours have spatial orientation, the on- & off-surface constraint points are not sensitive to spatial orientation. This is why our new reconstruction method can deal with arbitrarily oriented and mutually intersected contours, which is an important advantage of our approach.

- **Casting Surface reconstruction to equivalent variational problem:** After defining the constraints, the 3D surface reconstruction problem can be cast as the following scattered data interpolation problem:

Scattered data interpolation problem: Given a set of constraint points $\{ci\ (c^x_i, c^y_i, c^z_i)/^n_1\} \cap R^3$ and a set of their corresponding scalar values $\{h|^n_1\} \cap R$, find a function $f: R^3 \rightarrow R$ as the surface reconstruction result, so that:

$$f(c_i) = h_i\ (i = 1, \ldots, n) \quad (2)$$

But because the contours are very sparse, a direct interpolation can't lead to an ideal reconstruction result. One solution is to introduce an extra constraint to confine the scattered data interpolation problem. We use the following energy function as the extra constraint:

$$E(f) = \int_\Omega [f^2_{xx}(x) + f^2_{yy}(x) + f^2_{zz}(x) + 2(f^2_{xy}(x) + f^2_{yz}(x) + f^2_{zx}(x))]d\Omega \quad (3)$$

This energy function is basically a measure of the aggregate curvature of f(x) over the region of interest Ω and any creases or pinches in a surface will result in a larger value of the energy measure. So it indicates the smoothness of f(x). The more smooth is f(x), the smaller is E. Because medical anatomic structures are usually smooth, E(f) should be as small as possible.

With the energy measure, the surface reconstruction problem can be again cast to the following equivalent variational problem:

Equivalent variational problem: Given a set of constraint points $\{ci\ (c^x_i, c^y_i, c^z_i)/^n_1\} \cap R^3$ and a set of their corresponding scalar values $\{h|^n_1\} \cap R$, find a function $f: R^3 \rightarrow R$ as the surface reconstruction result, so that energy measure E(f) has the smallest value and:

$$f(c_i) = h_i\ (i = 1, \ldots, n) \quad (4)$$

The introduction of energy measure and casting of surface reconstruction problem to its equivalent variational problem makes our new reconstruction method capable of reconstructing an ideal smooth surface from very sparse contours. A very small number of contours will lead to excellent reconstruction result.

- **Variational interpolation: solution to equivalent variational problem:** In order to solve the equivalent variational problem, we first expand f(x) as the weighted sums of a RBF (radial basis function) Ø(x):

$$f(\mathbf{x}) = \sum_{j=1}^{n} d_j \phi(\mathbf{x} - \mathbf{c}_j) + P(\mathbf{x}) \quad (5)$$

In (5), c_i are the locations of the on- and off-surface constraints, dj are the weights. P(x) is a degree one polynomial that accounts for the linear and constant portions of f(x).We use the triharmonic spline for Ø(x), which is another commonly used 3D RBF, since it results in a C2-continuous and thus smoother interpolation (Rohr, 2001). It is defined by:

$$\phi(x) = \|x^3\| \quad (6)$$

Because the variational radial basis function naturally minimizes the energy measure (Turk *et al*., 2001), determining the weights dj and the coefficients of P(x) so that all the interpolation constraints are satisfied will yield the desired solution that minimizes the energy measure subject to the constraints.

Now substitute the constraints into equation (5), which gives:

$$h_i = \sum_{j=1}^{n} d_j \phi(\mathbf{c}_i - \mathbf{c}_j) + P(\mathbf{c}_i) \qquad (i = 1, \cdots, n) \quad (7)$$

Equation (7) can be formulated as a linear system. Let $\phi_{ij} = \phi(C_i - C_j)$, this linear system can be written as the following matrix form:

$$\begin{bmatrix} \phi_{11} & \phi_{12} & \dots & \phi_{1n} & 1 & c_1^x & c_1^y & c_1^z \\ \phi_{21} & \phi_{22} & \dots & \phi_{2n} & 1 & c_2^x & c_2^y & c_2^z \\ \dots & \dots & \dots & \dots & \dots & \dots & \dots & \dots \\ \phi_{n1} & \phi_{n2} & \dots & \phi_{nn} & 1 & c_n^x & c_n^y & c_n^z \\ 1 & 1 & \dots & 1 & 0 & 0 & 0 & 0 \\ c_1^x & c_2^x & \dots & c_n^x & 0 & 0 & 0 & 0 \\ c_1^y & c_2^y & \dots & c_n^y & 0 & 0 & 0 & 0 \\ c_1^z & c_2^z & \dots & c_n^z & 0 & 0 & 0 & 0 \end{bmatrix} \begin{bmatrix} d_1 \\ d_2 \\ \dots \\ d_n \\ p_0 \\ p_1 \\ p_2 \\ p_3 \end{bmatrix} = \begin{bmatrix} h_1 \\ h_2 \\ \dots \\ h_n \\ 0 \\ 0 \\ 0 \\ 0 \end{bmatrix} \quad (8)$$

According to Turk and Brien, the above system is symmetric and positive semi-definite, so there will always be a unique solution for dj and coefficients of P(x) (Turk *et al*., 2001). Solving it will gives us f(x) and a surface-extraction from f(x) will give us the reconstructed surface.

EXPERIMENTS AND DISCUSSION

Two experiments are conducted to evaluate our new surface reconstruction method, one using synthetic data, the other using phantom ultrasound data.

For phantom ultrasound image acquisition, we use a ZK-3000 ultrasound machine with a 3.5 MHz ultrasound probe (Beijing Zhongke-Tianli Tech. Co., Ltd., Beijing, China). The electromagnetic tracking device is the AURORA from Northern Digital Inc. (Ontario, Canada, http://www.ndigital.com). The digital ultrasound image is acquired through an image-grabbing card. As mentioned above, the position and orientation of the ultrasound probe is also recorded simultaneously using the tracking device (Fig. 3).

The 3D image reconstruction and visualization is performed using a personal computer with a 2.66 GHz Intel Core2™ quad CPU. We have developed IGS (image-guided surgery) software for microwave ablation of hepatic tumor (Fig. 4), which we uses as the surface reconstruction and visualization program in this study.

- **Experiment 1-using synthetic data:** In this experiment, we reconstruct a shelly object from several non-parallel cross-sections. The original data (Fig. 5a) is from the Amira Demos 3.1 CD (http://www.amiravis.com). 2, 4, 9, or 16 mutually intersected cross-sections are first re-sampled from the original data and are used respectively to reconstruct the shell. The experiment result is shown in Fig. 5. For each case, from left to right is: the used cross-sections, the boundary constraints (red) and their corresponding normal constraints (yellow), the reconstruction result, the visual difference between the reconstruction result (red) and the original data (yellow). The quantitative difference between the volume of the reconstruction result and the original data is illustrated in Table 1.

All the cross-sections are non-parallel to each other; actually they are intersecting each other. This indicates that our new method can handle arbitrarily oriented cross-sections. For all the cases, the new method gets good performance: the visual difference is small and the volume difference is no more than 1.5%. Furthermore, the new method takes a small number of cross-sections as input data, even two cross-sections can lead to a close approximation of the original data. As the number of used cross-sections increases, the volume difference doesn't decrease drastically accordingly. Actually, a

Fig. 3: Phantom experiment configuration

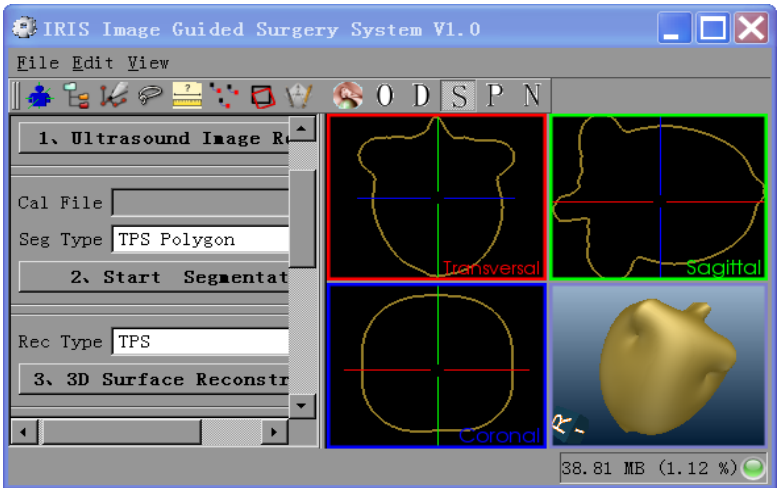

Fig. 4: Reconstruction and visualization software

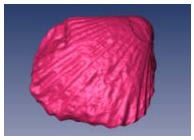

(a)

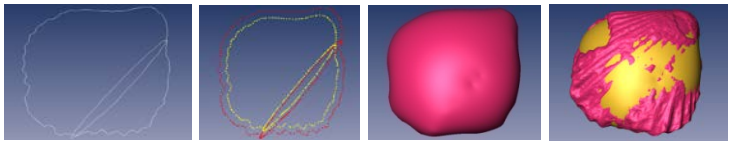

(b)

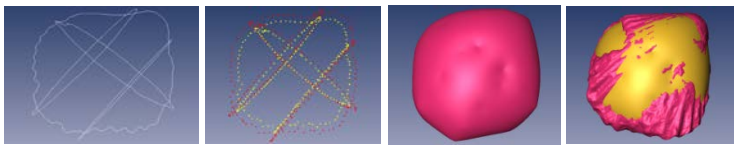

(c)

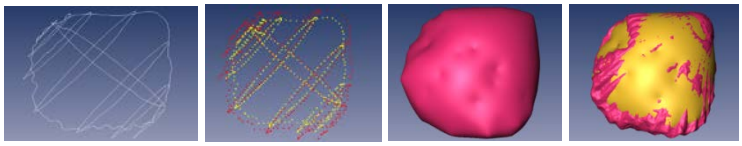

(d)

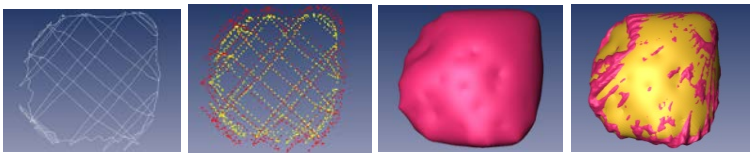

(e)

Fig. 5: Surface reconstruction of a shell using synthetic data, (a) Original data; (b) 2 slices; (c) 4 slices; (d) 9 slices; (e) 16 slices

Table 1: Volume difference between reconstructed surface and original data (shell)

Number of cross sections	Volume (mm^3)	Volume difference (mm^3)	Volume difference (%)
Original data	1529.90		
2	1523.63	-6.27	-0.41
4	1505.09	-20.81	-1.36
9	1545.96	20.06	1.31
16	1547.09	21.19	1 .39

Table 2: Volume difference between reconstructed surface and original data (plastic apple)

Number of cross sections	Volume (mm^3)	Volume difference (mm^3)	Volume difference (%)
Original data	183300		
3	202230	18930	10.33
4	197588	14288	7.80
7	194807	11507	6.28

(a)

(b)

(c)

(d)

Fig. 6: Surface reconstruction of a toy apple using phantom ultrasound data, (a) Original data; (b) 3 slices; (c) 4 slices; (d) 7 slices

great many number of cross-sections will lead to large computation overhead and makes our new method no more feasible for real-time reconstruction.

There are many creases and pinches in the surface of the original data, these details are missing in the reconstruction result. This is because that VIF reconstruction method should minimize the energy measure and any creases or pinches in a surface will result in a larger value of the energy measure. For clinical applications, this problem doesn't matter much because most surfaces of the anatomic structures are smooth.

- **Experiment 2 - using phantom ultrasound data:** In this experiment, we reconstruct a phantom from real ultrasound data. The phantom we used is a plastic apple (Fig. 6a). 3, 4, or 7 mutually intersected cross-sections are used respectively to reconstruct the apple. The experiment result is shown in Fig. 6. For each case, from left to right is: the original ultrasound data and segmented contours (light blue), the used cross-sections and the reconstruction result. The quantitative difference between the volume of the reconstruction result and the original phantom data is illustrated in Table 2.

The result of this experiment conforms to that of experiment 1. Visually all the reconstruction surfaces resemble to the original plastic apple in an amazing way. The volume difference is a little bigger than that of experiment 1, which may result from the inaccuracy of the volume measurement of the original plastic apple, but still in an acceptable limit.

CONCLUSION

We present a new approach for the surface reconstruction of sparse and mutually-intersected contours in freehand 3D ultrasound imaging based on variational interpolation. It is capable of creating smooth surface from a small number of segmented contours which can be arbitrarily oriented in 3D space, that is, it can handle both sparse and non-parallel contours which are two main drawbacks of freehand 3D ultrasound imaging and have disabled many conventional 3D reconstruction method

Two experiments are conducted to evaluate the new surface reconstruction method, one using synthetic data, the other using phantom ultrasound data. The results have shown that new method can get good performance: the visual difference and the volume difference between the reconstruction result and the original data is very small, even two contours can lead to a close approximation of the original data. These results also confirm that our reconstruction method can handle both sparse and mutually-intersected contours.

The reconstructed surface produced by the new method appears smooth and natural. This problem doesn't matter much because objects in medical images are rather smooth as biological structures generally do not have sharp edges.

ACKNOWLEDGMENT

The study was supported by the Science and Technology Plan sponsored by Beijing Municipal Science and Technology Commission under the Key Project grant H060720050330 and supported by the Science and Technology Plan sponsored by Beijing Municipal Commission of Education under grant 08010921003 and supported by Funding Project for Academic Human Resources Development in Institutions of Higher Learning Under the Jurisdiction of Beijing Municipality.

REFERENCES

Altmann, K., Z. Shen, L.M. Boxt, D.L. King, W.M. Gersony, L.D. Allan and H.D. Apfel, 1997. Comparison of three-dimensional echocardiographic assessment of volume, mass and function in children with functionally single left ventricles with two-dimensional echocardiography and magnetic resonance imaging. Am. J. Cardiol., 80: 1060-1065.

Barry, C.D., C.P. Allott, N.W. John, P.M. Mellor, P.A. Arundel, D.S. Thomson and J.C. Waterton, 1997. Three dimensional freehand ultrasound: Image reconstruction and volume analysis. Ultrasound Med. Biol., 23(8): 1209-1224.

Cook, L.T., P.N. Cook, L.K. Rak, S. Batnitzky, B.Y.S. Wong, S.L. Fritz *et al*., 1980. An algorithm for volume estimation based on polyhedral approximation. IEEE T. Biomed. Eng., 27: 493-500.

Fenster, A. and D.B. Downey, 1996. 3-D ultrasound imaging: A review. IEEE Eng. Med. Biol. Mag., 15(6): 41-51.

Gopal, A.S., M.J. Schnellbaecher, Z. Shen, O.O. Akinboboye, P.M. Sapin and D.L. King, 1997. Freehand three-dimensional echocardiography for measurement of left ventricular mass: In vivo anatomic validation using explanted human hearts. J. Am. Coll. Cardiol., 30: 802-810.

Hodges, T.C., P.R. Detmer, D.H. Burns, K.W. Beach and D.E. Jr Strandness, 1994. Ultrasonic three-dimensional reconstruction: In vitro and in vivo volume and area measurement. Ultrasound Med. Biol., 20: 719-729.

King, D.L., A.S. Gopal, A.M. Keller, P.M. Sapin and K.M. Schr¨oder, 1994. Three-dimensional echocardiography: Advances for measurement of ventricular volume and mass. Hypertension, 23: I-172-I-179.

Liu, L., C. Bajaj, J.O. Deasy, D.A. Low and T. Ju, 2008. Surface reconstruction from non-parallel curve networks. Comput. Graph. Forum, 27(2): 155-163.

Nelson, T.R. and D.H. Pretorius, 1997. Interactive acquisition, analysis and visualization of sonographic volume data. Int. J. Imag. Syst. Technol., 8(1997): 26-37.

Prager, R.W., A.H. Gee and L. Berman, 1999. Stradx: Real-time acquisition and visualization of freehand three-dimensional ultrasound. Med. Image Anal., 3(2): 129-140.

Rohr, K., 2001. Landmark-based Image Analysis: Using Geometric and Intensity Models. Springer, Netherlands, ISBN: 0792367510.

Rousseau, F., P. Hellier and C. Barillot, 2005. Confhusius: A robust and fully automatic calibration method for 3D freehand ultrasound. Med. Image Anal., 9(2005): 25-38.

Rousseau, F., P. Hellier and C. Barillot, 2006. A novel temporal calibration method for 3-D ultrasound. IEEE T. Med. Imag., 25(8): 1108-1112.

Sherebrin, S., A. Fenster, R.N. Rankin and D. Spence, 1996. Freehand three-dimensional ultrasound: Implementation and applications. In: Richard L. Van Metter, Jacob Beutel (Eds.), Proceeding of the SPIE, Physics of Medical Imaging, 2708: 296-303.

Trobaugh, J.W., D.J. Trobaugh and W.D. Richard, 1994. Three dimensional imaging with stereotactic ultrasonography. Comput. Med. Imag. Graph., 18(5): 315-323.

Turk, G., H.Q. Dinh, J. O'Brien and G. Yngve, 2001. Implicit surfaces that interpolate. Proceeding of the International Conference on Shape Modeling and Applications, IEEE Computer Society, pp: 62-71.

William, E.L. and E.C. Harvey, 1987. Marching cubes: A high resolution 3D surface construction algorithm. Comput. Graph. (SIGGRAPH 87), 21(4): 163-169.